arXiv:0909.5689v1 [hep-ex] 30 Sep 2009

Model-Independent Results for the Decay $B^+ \to \ell^+\nu_\ell\gamma$ at BABAR

D. M. Lindemann *(On behalf of the BABAR Collaboration)*
Department of Physics, McGill University, Montréal, Québec, Canada H3A 2T8

We present a search for the radiative leptonic decays $B^+ \to e^+\nu_e\gamma$ and $B^+ \to \mu^+\nu_\mu\gamma$ using data collected by the BABAR detector at the PEP-II B factory. We fully reconstruct the hadronic decay of one of the B mesons in $\Upsilon(4S) \to B^+B^-$ and then search for evidence of the signal decay within the rest of the event. This method provides clean kinematic information on the signal's missing energy and high momentum photon and lepton, and allows for a model-independent analysis of this decay. Using a data sample of 465 million B-meson pairs, we obtain sensitivity to branching fractions of the same order as predicted by the Standard Model. We report a model-independent branching fraction upper limit of $\mathcal{B}(B^+ \to \ell^+\nu_\ell\gamma) < 15.6 \times 10^{-6}$ ($\ell = e$ or μ) at the 90% confidence level.

1. Introduction

The leptonic decay $B^+ \to \ell^+\nu_\ell\gamma$, where $\ell = e$ or μ, proceeds via an annihilation of b and u quarks into a virtual W^+ boson with the radiation of a photon.[1] Leptonic decays can provide clean theoretical predictions of Standard Model (SM) parameters without the QCD-based uncertainties arising from hadrons in the final state. The purely leptonic decay $B^+ \to \ell^+\nu_\ell$, which offers a clean prediction of the B-meson decay constant f_B, is helicity suppressed, having a branching fraction that is proportional to the square of the lepton mass. Although the radiative mode is additionally suppressed by a factor $\alpha_{\rm em}$, the presence of the photon can remove the helicity suppression by affecting the coupling of the spin-0 B meson to the spin-1 $W^\pm$ boson, possibly through an intermediate off-shell state [1]. The branching fraction of $B^+ \to \ell^+\nu_\ell\gamma$ is predicted in the SM to be independent of the lepton type and of order 10^{-6}, making it potentially accessible at current and future B factories such as BABAR and SuperB [2] respectively. The most stringent published limits are from the CLEO collaboration with $\mathcal{B}(B^+ \to e^+\nu_e\gamma) < 2.0 \times 10^{-4}$ and $\mathcal{B}(B^+ \to \mu^+\nu_\mu\gamma) < 5.2 \times 10^{-5}$ at the 90% confidence level (CL) [3].

The branching fraction of the signal decay can be written as [4]:

$$\mathcal{B}(B^+\to \ell^+\nu_\ell\gamma) = \frac{\alpha G_F^2}{288\pi^2}|V_{ub}|^2 f_B^2 m_B^5 \tau_B \left(\frac{Q_u}{\lambda_B} - \frac{Q_b}{m_b}\right)^2 \tag{1}$$

where G_F is the Fermi constant, V_{ub} is the Cabibbo-Kobayashi-Maskawa (CKM) matrix element describing the coupling of b and u quarks, m_B and τ_B are the B-meson mass and lifetime respectively, Q_i is the quark charge, and λ_B is the first inverse moment of the light-cone B-meson wave function. This last parameter plays an important role in proving QCD factorization [5]. It also enters into calculations of the $B \to \pi$ form factor at zero momentum transfer and the branching fractions of two-body hadronic B-meson decays such as $B \to D\pi$ and $B \to \pi\pi$ [6], the latter being a benchmark channel for measuring the angle α of the CKM Unitarity Triangle. Typically assumed to be of order Λ_{QCD}, at a few hundred MeV, λ_B currently suffers from significant theoretical uncertainty [7]. A measurement of $\mathcal{B}(B^+ \to \ell^+\nu_\ell\gamma)$ can provide a clean prediction of this important parameter. In addition, since $B^+ \to \ell^+\nu_\ell\gamma$ is a possible background for $B^+ \to \ell^+\nu_\ell$, a measurement of $\mathcal{B}(B^+ \to \ell^+\nu_\ell\gamma)$ over the full photon energy spectrum is needed for an accurate measurement of $\mathcal{B}(B^+ \to \ell^+\nu_\ell)$ [8], which would improve predictions of f_B.

2. Analysis

This analysis uses data taken from the BABAR experiment [9], located at the asymmetric-energy PEP-II e^+e^- storage rings at SLAC in California. On-peak data is produced by colliding electrons and positrons with a center-of-mass (CM) energy at the $\Upsilon(4S)$ resonance of 10.58 GeV, just above the threshold for $B\overline{B}$ production. We use the full BABAR dataset of 465 ± 5 million B-meson pairs, corresponding to an integrated luminosity of 423 fb^{-1}. Charged-particle momenta are measured using a tracking system comprised of a silicon vertex detector and drift chamber contained within the uniform magnetic field of a 1.5T superconducting solenoid. Charged-particle identification is based on the energy loss in the tracking system and the Cherenkov angle in a ring-imaging Cherenkov detector. Photon energies and electron identification are provided by a CsI(Tl) scintillating electromagnetic calorimeter (EMC). Finally, muons are distinguished from hadrons using instrumentation embedded within the steel magnetic-flux return. Monte Carlo (MC) simulations are used to model the detector response, determine the signal efficiency, and study the background.

---

[1] Charge conjugate modes are included implicitly throughout this paper.

2.1. Hadronic Reconstruction

We present the first search for $B^+ \to \ell^+\nu_\ell\gamma$ that uses an exclusive method, by fully reconstructing one B meson ($B_{\rm tag}$) via hadronic decay modes. Unlike previous inclusive searches of $B^+ \to \ell^+\nu_\ell\gamma$, which identified the signal lepton and photon candidates before the recoiling B meson, we reconstruct the recoil B meson first before searching for the signal decay. Although this technique results in a low signal efficiency (0.3% for signal modes), and thus more statistically-limited results, it compensates by providing a highly pure sample of B mesons with comparatively little non-$B\overline{B}$ (continuum) background. Our reliance on poorly-modeled continuum background is thus reduced, which enables a search for $B^+ \to \ell^+\nu_\ell\gamma$ that can avoid kinematic constraints in the signal selection. Therefore, we present the first model-independent search of $\mathcal{B}(B^+ \to \ell^+\nu_\ell\gamma)$ over the full kinematic range. In addition, by reconstructing the $B_{\rm tag}$ using only detectable hadronic decay modes, the missing four-vector of the otherwise undetectable signal neutrino is fully determined.

The event selection begins by reconstructing a $D^{(*)}$ meson using various hadronic decay modes, listed in Ref. [10]. Additional charged tracks and neutral EMC clusters are then combined with the $D^{(*)}$ seed to form the decay $B \to D^{(*)}X_{\rm had}$, where $X_{\rm had}$ is a combination of neutral and charged pions and/or kaons. $X_{\rm had}$ is chosen such that $|\Delta E| \equiv |E_{B_{\rm tag}} - \frac{\sqrt{s}}{2}| < 0.12$, where $\sqrt{s}$ is the total energy of the e^+e^- system and $E_{B_{\rm tag}}$ is the $B_{\rm tag}$ candidate energy, both in the CM frame. If there exists more than one $B_{\rm tag}$ candidate, we choose the one with the $D^{(*)}$ and $X_{\rm had}$ mode that provides the highest purity of well-reconstructed candidates. Finally, we require that the $B_{\rm tag}$ candidate is charged.

Since the beam energy at PEP-II is accurately known within a few MeV, we define the mass of the $B_{\rm tag}$ as $m_{\rm ES} = \sqrt{\frac{s}{4} - \vec{p}^{\,2}_{B_{\rm tag}}}$, where $\vec{p}_{B_{\rm tag}}$ is the $B_{\rm tag}$ three-momentum in the CM frame. Since the $B_{\rm tag}$ candidate should have a mass consistent with the nominal B-meson mass, we require $5.27 < m_{\rm ES} < 5.29\,{\rm GeV}/c^2$. The $m_{\rm ES}$ sideband region, defined as $5.20 < m_{\rm ES} < 5.26\,{\rm GeV}/c^2$, is populated by combinatoric background, events coming from a $\Upsilon(4S) \to B\overline{B}$ or continuum decay in which the $B_{\rm tag}$ is incorrectly reconstructed. To improve the MC estimation of the reconstruction efficiency, we normalize the MC that peaks within the $m_{\rm ES}$ signal region to the data that peaks within this same region, after applying the $B_{\rm tag}$ selection criteria. In addition, we reduce our reliance on the MC estimate of combinatoric events by estimating the non-peaking background directly from the data within the $m_{\rm ES}$ sideband.

When a $\Upsilon(4S)$ resonance decays to a $B\overline{B}$ pair, the two particles are almost at rest, with a momenta of about $350\,{\rm MeV}/c$ in the CM frame, since their masses are about half the $\Upsilon(4S)$ mass. Therefore, they tend to decay with an isotropically symmetric topology in the CM frame. On the other hand, lighter $q\overline{q}$ and $\tau^+\tau^-$ pairs, which are also produced in the e^+e^- interactions, have a higher momentum in the CM frame. Their decays tend to have a more jet-like shape with a strongly-preferred direction characterizing the event, preferentially at small angles in relation to the beam axis. Therefore, to achieve a higher purity of B mesons, we use a multivariate selector of five event-shape variables to separate $B\overline{B}$ from continuum events. We require:

$$\mathcal{L}_B \equiv \frac{\prod_i \mathcal{P}_B(x_i)}{\prod_i \mathcal{P}_B(x_i) + \prod_i \mathcal{P}_q(x_i)} > 30\%, \qquad (2)$$

where $\mathcal{P}_B(x_i)$ and $\mathcal{P}_q(x_i)$ are probability density functions determined from MC that describe $B\overline{B}$ and continuum events, respectively, for the five event-shape variables x_i. These variables, as explained in Ref. [10], describe the sphericity of the event, the magnitude and directions of the thrust axes, and the direction of the $B_{\rm tag}$ momentum with respect to the beam axis. This requirement also suppresses the poorly-modeled continuum backgrounds which can contribute to discrepancies between the MC and data.

2.2. Signal Selection

After the $B_{\rm tag}$ reconstruction, we assign all the remaining charged tracks and neutral EMC clusters, to the signal B meson ($B_{\rm sig}$), as well as any missing momentum ($\vec{p}_{\rm miss}$) within the event. We require that $B_{\rm sig}$ has exactly one track, with a charge opposite that of the $B_{\rm tag}$ charge. In addition, this signal track must satisfy particle identification criteria of either an electron or muon and fail that of a kaon.

Because high energy electrons can emit bremsstrahlung photons, we search for signal-side clusters that have proximity to the EMC deposit of an electron candidate, both in θ, the angle from the beam axis, and in ϕ, the azimuthal angle around the beam axis. Because the detector has a solenoid magnet through which all the particles travel, charged particles are bent in ϕ according to their charge, and therefore $\Delta\phi$ is multiplied by the lepton candidate charge. Any cluster with a momentum vector that is separated from that of the electron-identified signal track by $|\Delta\theta| < 3^\circ$ and $-3^\circ < \Delta\phi < 13^\circ$ is identified as a bremsstrahlung photon. The energy of this cluster is then used to correct the four-vector of the signal track (p_ℓ) and is removed from the list of clusters. Next, we identify the signal photon candidate, whose energy spectrum is expected to peak around 1 GeV. We do this by searching through the remaining signal-side clusters for the one with the highest energy in the CM frame.

Although $B^+ \to \ell^+\nu_\ell\gamma$ should only have one signal-side cluster if correctly reconstructed, extra clusters within an event can be due to fragments from particle showers, low-energy clusters from the $B_{\rm tag}$, and/or noise in the detector such as beam-related photons. Because of the presence of extra clusters, we apply the very loose requirement that there are no more than 11 additional low energy clusters which are not otherwise used in the $B_{\rm tag}$ or signal reconstruction. The total energy of these clusters is required to be less than 800 MeV, where we only include in this sum clusters which have lab-frame energy greater than 50 MeV.

Missing energy can be due to either an undetectable particle such as a neutrino or a detectable particle that travels outside of the fiducial acceptance of the detector. To suppress events of the latter category, we require that $\vec{p}_{\rm miss}$ points within the fiducial acceptance of the detector.

The lepton and neutrino are produced back-to-back by the virtual $W^\pm$ boson. However, in the $B_{\rm sig}$ rest frame, the angle $\theta_{\ell\nu}$ between the signal track momentum and $\vec{p}_{\rm miss}$ is affected by the release of the photon. Therefore, we require $\cos\theta_{\ell\nu} < -0.93$ in the frame recoiling from the photon. This frame is defined as the difference between the $B_{\rm sig}$ four-vector (p_B) and the signal photon candidate four-vector (p_γ). Including this requirement assures that the decay is consistent with being a three-body decay, independent of when the photon was released.

The most discriminating variable in this analysis is a requirement on the neutrino candidate's invariant mass m_ν^2, given by:

$$m_\nu^2 = (p_B - p_\gamma - p_\ell)^2. \tag{3}$$

This requirement isolates events in which the photon and lepton candidates are in kinematic agreement with a massless third daughter in the event. Fig. 1 shows that the signal peaks at zero, while the the background rises with m_ν^2. The tail on the signal distribution is larger for the electron mode than the muon mode due to unrecovered bremsstrahlung photons. The signal region for this variable is defined as $-1 < m_\nu^2 < 0.46\ (0.46)\ {\rm GeV}^2/c^4$ for the electron (muon) mode. These values, as with all other cut values in this analysis, were optimized using the figure of merit $\varepsilon_\ell^{\rm sig}/(\frac{1}{2}n_\sigma + \sqrt{N_\ell^{\rm bkg}})$ [11], where $n_\sigma = 1.3$, $\varepsilon_\ell^{\rm sig}$ is the total signal efficiency, and $N_\ell^{\rm bkg}$ is the number of expected background events.

The m_ν^2 and $\cos\theta_{\ell\nu}$ requirements kinematically restrict the types of events that pass. Since light X_u mesons often decay to a pair of photons, where X_u is a neutral meson containing a u-quark, the topology and kinematics of a $B^+ \to X_u^0\ell^+\nu_\ell$ event can often mimic that of the signal decay. This is particularly true if one photon is "missing" such as through misreconstruction into the $B_{\rm tag}$ or due to a lab-frame energy that is too low to be detectable by the EMC. Thus, the primary background that passes the signal selection are $B^+ \to X_u^0\ell^+\nu_\ell$ events with a high energy photon. To suppress $B^+ \to X_u^0\ell^+\nu_\ell$ events in which both photon daughters are present in the signal-side clusters, we reject events in which the signal photon candidate can be combined with another cluster to form an invariant mass consistent with the π^0 or η mass. To improve the purity of the reconstructed π^0 mesons, we only use clusters that are above a given energy $E_{\gamma2}$ in the $B_{\rm sig}$ rest frame. To suppress $B^+ \to \pi^0\ell^+\nu_\ell$ events, we reject events in which the invariant mass is between 120 and 145 MeV with $E_{\gamma2} > 30$ MeV or between 100 and 160 MeV with $E_{\gamma2} > 80$ MeV. Since η particles are much more massive and thus tend to decay into higher energy photons, we suppress $B^+ \to \eta\ell^+\nu_\ell$ events by rejecting events with $E_{\gamma2} > 100MeV$ and an invariant mass between 515 and 570 MeV. Finally, we suppress $B^+ \to \omega\ell^+\nu_\ell \to [\pi^0\gamma]\ell^+\nu_\ell$ events by rejecting events in which the signal photon candidate combined with a π^0 candidate forms an invariant mass between 115 and 145 MeV. This π^0 candidate must have $E_{\gamma2} > 70$ MeV and an invariant mass between 115 and 145 MeV.

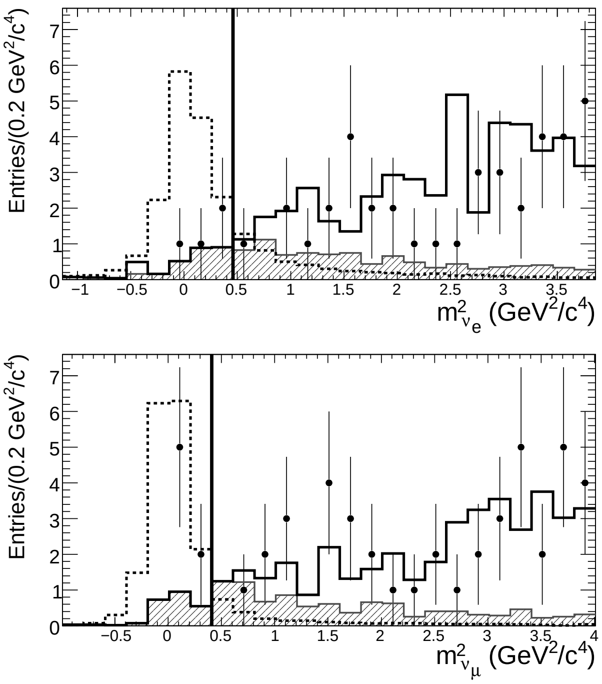

Figure 1: m_ν^2 distribution after all selection criteria are applied, in electron (top) and muon (bottom) modes for the $m_{\rm ES}$-peaking (shaded) plus non-peaking (solid) contributions in the full background MC sample, signal MC normalized to $\mathcal{B} = 40\times10^{-6}$ (dashed), and data (points). Events to the left of the vertical lines are selected.

Events in which the two photons from a $B^+ \to \pi^0\ell^+\nu_\ell$ decay are merged into a single EMC cluster can mimic the signal kinematics exactly, since the cluster chosen as the signal photon candidate contains the full energy of the π^0. We suppress this background using a requirement on the cluster width of the signal photon candidate. A cluster that is the result of two merged photons from a π^0 decay tends to be wider than a cluster from a single photon. We require the lateral moment [12] to be less than 55%.

2.3. Backgrounds and Uncertainties

We define the signal branching fraction for each lepton mode ℓ as:

$$\mathcal{B}_\ell = \frac{N_\ell^{\rm obs} - N_\ell^{\rm bkg}}{\varepsilon_\ell^{\rm sig} N_{B^\pm}} \tag{4}$$

where $N_\ell^{\rm obs}$ is the number of observed data events within the signal region and $N_{B^\pm} = 465 \times 10^6$ is the number of $B^\pm$ mesons in the data sample. The branching fractions are computed using the frequentist formalism of Feldman and Cousins [13], with uncertainties on $N_\ell^{\rm bkg}$ and $\varepsilon_\ell^{\rm sig}$ modeled using Gaussian distributions. Since $\mathcal{B}(B^+ \to \ell^+\nu_\ell\gamma)$ is expected to be independent of the lepton type, we also combine the branching fractions of the two modes.

The MC indicates that the selection criteria, especially the one track requirement and the m_ν^2 and $\cos\theta_{\ell\nu}$ restrictions on the event kinematics, removes all decay types except $B^+ \to X_u^0\ell^+\nu_\ell$ events and the occasional combinatoric event from a misreconstructed $B_{\rm tag}$. Thus, we split $N_\ell^{\rm bkg}$ into two categories: peaking events ($N_\ell^{\rm peak}$) and combinatoric events ($N_\ell^{\rm comb}$). An event is considered peaking if it comes from a $\Upsilon(4S) \to B\overline{B}$ decay in which the $B_{\rm tag}$ is correctly reconstructed and hence peaks within the $m_{\rm ES}$ signal region. Since only $B^+ \to X_u^0\ell^+\nu_\ell$ events peak in this region, we improve the statistics of $N_\ell^{\rm peak}$ by using exclusive $B^+ \to X_u^0\ell^+\nu_\ell$ MC samples. For $N_\ell^{\rm comb}$, we extrapolate the number of misreconstructed $B_{\rm tag}$ events in the $m_{\rm ES}$ signal region directly from the number of data events in the $m_{\rm ES}$ sideband.

The uncertainty on $N_\ell^{\rm comb}$ is dominated by the sideband data statistics, but it also includes a 14.6% systematic uncertainty on the $m_{\rm ES}$ combinatoric background shape. On the other hand, since $\varepsilon_\ell^{\rm sig}$ and $N_\ell^{\rm peak}$ rely on the accuracy of the MC simulations, their uncertainties arise not only from MC statistics, but also include systematic uncertainties due to how well the MC agrees with the data. The contributions to the systematic uncertainties are listed in Table I. The systematic uncertainty of $N_\ell^{\rm peak}$ is dominated by a 13.6% uncertainty in the branching fractions and form factors of various exclusive $B^+ \to X_u^0\ell^+\nu_\ell$ decays [10]. The uncertainty due to the $B_{\rm tag}$ reconstruction, which also accounts for the uncertainty in $N^{B^\pm}$, is determined by varying the shape and scaling of the $m_{\rm ES}$ combinatoric distribution.

Table I Contributions (in percent) to the systematic uncertainty on the branching fraction due to the signal efficiency $\varepsilon_\ell^{\rm sig}$ and the peaking-background estimate $N_\ell^{\rm peak}$. The $\mathcal{B}(B^+ \to X_u^0\ell^+\nu_\ell)$ source refers to branching fraction and form factor uncertainties in $B^+ \to X_u^0\ell^+\nu_\ell$ decays.

Source of	$\varepsilon_\ell^{\rm sig}$		$N_\ell^{\rm peak}$	
systematics	e mode	μ mode	e mode	μ mode
$\mathcal{B}(B^+ \to X_u^0\ell^+\nu_\ell)$	–	–	13.6	13.6
$B_{\rm tag}$ reconstruction	3.1	3.1	3.1	3.1
Particle identification	0.9	1.3	0.9	1.3
Track reconstruction	0.4	0.4	0.4	0.4
Photon reconstruction	1.8	1.8	1.8	1.8
$\mathcal{L}_B$	1.4	1.4	1.4	1.4
m_ν^2	0.5	0.5	1.4	1.4

3. Results

To avoid experimenter bias, we blinded the data in the region $m_\nu^2 < 1\,{\rm GeV}^2/c^4$ and $m_{\rm ES} > 5.26\,{\rm GeV}/c^2$ until all selection criteria, background estimates, and systematic uncertainties were finalized. The final signal efficiencies correspond to approximately one signal event per mode, assuming a branching fraction within the SM predictions. After unblinding, we observe 4 (7) data events within the signal region for the electron (muon) mode, compared to an expected background of 2.7 ± 0.6 (3.4 ± 0.9) events. The branching fraction results are given in Table II.

Table II Expected background yields $N_\ell^{\rm bkg} = N_\ell^{\rm comb} + N_\ell^{\rm peak}$, signal efficiencies $\varepsilon_\ell^{\rm sig}$, number of observed data events $N_\ell^{\rm obs}$, resulting branching fraction limits at 90% CL, and the combined central value $\mathcal{B}_{combined}$. Uncertainties are given as statistical ± systematic.

	$B^+ \to e^+\nu_e\gamma$	$B^+ \to \mu^+\nu_\mu\gamma$
$N_\ell^{\rm comb}$	$0.3 \pm 0.3 \pm 0.1$	$1.2 \pm 0.6 \pm 0.6$
$N_\ell^{\rm peak}$	$2.4 \pm 0.3 \pm 0.4$	$2.1 \pm 0.3 \pm 0.3$
$N_\ell^{\rm bkg}$	$2.7 \pm 0.4 \pm 0.4$	$3.4 \pm 0.7 \pm 0.7$
$\varepsilon_\ell^{\rm sig}$	$(7.8 \pm 0.1 \pm 0.3)\times10^{-4}$	$(8.1 \pm 0.1 \pm 0.3)\times10^{-4}$
$N_\ell^{\rm obs}$	4	7
$\mathcal{B}_{combined}$	$\left(6.5^{+7.6+2.8}_{-4.7-0.8}\right) \times 10^{-6}$	
Model-ind.	$< 17\times10^{-6}$	$< 26\times10^{-6}$
Limits	$< 15.6 \times 10^{-6}$	

Although the effective detector and particle identification thresholds are about 20 MeV for photon energy and 400 (800) MeV for electron (muon) momentum, and we apply no minimum energy requirements. Thus, this analysis is essentially valid over the full kinematic range, as shown in Fig. 2. However, there exists theoretical uncertainty in the photon energy spectrum below $\Lambda_{\rm QCD}$ for the $B^+ \to \ell^+\nu_\ell\gamma$ decay. Therefore, using certain theoretical techniques, the extraction of λ_B can be improved by including a minimum energy requirement on the signal photon [7]. When the signal photon candidate energy is required to be greater than 1 GeV, we observe 2 (4) data events with $N_\ell^{\rm bkg} = 1.4 \pm 0.3$ (2.5 ± 1.0) in the electron (muon) mode. The $\varepsilon_\ell^{\rm sig}$, which is mostly uncorrelated with the photon energy spectrum, is reduced by 30%, resulting in a partial branching fraction of $\Delta\mathcal{B}(B^+ \to \ell^+\nu_\ell\gamma) < 14 \times 10^{-6}$ at 90% CL.

The differential branching fraction versus photon energy E_γ of $B^+ \to \ell^+\nu_\ell\gamma$ is given by:

$$\frac{d\Gamma}{dE_\gamma} = \frac{\alpha G_F^2}{48\pi^2}|V_{ub}|^2 m_B^4 \left(f_A^2(E_\gamma) + f_V^2(E_\gamma)\right) x(1-x)^3 \tag{5}$$

where $y \equiv 2E_\gamma/m_B$. The two form factors, f_V and f_A, describe the vector and axial-vector contributions, respectively, to the $B \to \gamma$ transition. Although $f_A = 0$ in some models [1] and was assumed in the CLEO measurement of $\mathcal{B}(B^+ \to \ell^+\nu_\ell\gamma)$, most models assert $f_A = f_V$ [5]. In this analysis, we use signal MC that is generated based on the tree-level hadronic matrix element for $B^+ \to \ell^+\nu_\ell\gamma$ as described by Ref. [4], using a minimum photon energy of 350 MeV. We use both form-factor models for our signal MC to evaluate the impact of the decay model on the signal selection efficiency and to ensure model-independency. We determine $\varepsilon_\ell^{\rm sig}$ using the $f_A = f_V$ signal model, but because our analysis is independent of the decay kinematics, the $f_A = 0$ model yields consistent $\varepsilon_\ell^{\rm sig}$ values.

We also determine branching fraction limits that are dependent on the signal model by introducing a kinematic requirement on the angles between the three daughter particles of the signal decay. We use the quantities $\cos\theta_{\gamma\ell}$ and $\cos\theta_{\gamma\nu}$, where $\theta_{\gamma\ell}$ is the angle between the photon candidate and signal track momenta, and $\theta_{\gamma\nu}$ is the angle between the photon candidate momentum and $\vec{p}_{\rm miss}$, both in the $B_{\rm sig}$ rest frame. As seen in Fig. 3, the photon is emitted preferentially back-to-back with the lepton in the $f_A = f_V$ model, and back-to-back with either the lepton or neutrino in the $f_A = 0$ model. Thus, we require $(\cos\theta_{\gamma\ell}-1)^2+(\cos\theta_{\gamma\nu}+1)^2/3 > 0.4$ or $(\cos\theta_{\gamma\nu}-1)^2+(\cos\theta_{\gamma\ell}+1)^2/3 > 0.4$ for the $f_A = 0$ model, and only the former relationship for $f_A = f_V$. This reduces $\varepsilon_\ell^{\rm sig}$ in both modes and models by 40%. We observe 0 (0) data events in the electron (muon) mode with $N_\ell^{\rm bkg} = 0.6 \pm 0.1$ (1.0 ± 0.4) for the $f_A = f_V$ model, corresponding to $\mathcal{B}(B^+ \to \ell^+\nu_\ell\gamma) < 3.0 \times 10^{-6}$. Likewise, in the $f_A = 0$ model, we observe 3 (2) data events with $N_\ell^{\rm bkg} = 1.2 \pm 0.4$ (1.5 ± 0.6), corresponding to $\mathcal{B}(B^+ \to \ell^+\nu_\ell\gamma) < 18 \times 10^{-6}$.

4. Conclusion

In conclusion, we have searched for $B^+ \to \ell^+\nu_\ell\gamma$ using a hadronic recoil technique and observe no significant signal within a data sample of 465 million $B\overline{B}$ pairs. We report a model-independent limit of $\mathcal{B}(B^+ \to \ell^+\nu_\ell\gamma) < 15.6 \times 10^{-6}$ at the 90% CL, which is consistent with the standard model prediction and is the most stringent published upper limit to date. Using Eq. (1) with $f_B = 0.216 \pm 0.022\,\mathrm{GeV}$, $m_B = 5.279\,\mathrm{GeV}/c^2$, $\tau_B = 1.638$ ps, $m_b = 4.20\,\mathrm{GeV}/c^2$, and $|V_{ub}| = (3.93 \pm 0.36) \times 10^{-3}$ [14], the combined branching fraction likelihood function corresponds to a limit of $\lambda_B > 0.3\,\mathrm{GeV}$ at the 90% CL.

References

[1] G. Burdman, T. Goldman, and D. Wyler, Phys. Rev. D **51**, 111 (1995).

[2] SuperB Collaboration, SuperB Conceptual Design Report, arXiv:0709.0451v2 [hep-ex], (2007).

[3] CLEO Collaboration, T. E. Browder *et al.*, Phys. Rev. D **56**, 11 (1997).

[4] G. P. Korchemsky, D. Pirjol, and T. M. Yan, Phys. Rev. D **61**, 114510 (2000).

[5] E. Lunghi, D. Pirjol, and D. Wyler, Nucl. Phys. B **649**, 349 (2003); S. Descotes-Genon and C. T. Sachrajda, Nucl. Phys. B **650**, 356 (2003).

[6] A. Le Yaouanc, L. Oliver, and J.-C. Raynal, Phys. Rev. D **77**, 034005 (2008).

[7] P. Ball and E. Kou, JHEP **0304**, 29 (2003).

[8] D. Becirevic, B. Haas, and E. Kou, arXiv:0907.1845v1 [hep-ph], (2009).

[9] *BABAR* Collaboration, B. Aubert *et al.*, Nucl. Instr. Meth. A **479**, 1 (2002).

[10] *BABAR* Collaboration, B. Aubert *et al.*, arXiv:0907.1681 [hep-ex], submitted to Phys. Rev. D (RC), (2009).

[11] G. Punzi, arXiv:physics/0308063v2 [physics.data-an], (2003).

[12] ARGUS Collaboration, A. Drescher *et al.*, Nucl. Instr. Meth. A **237**, 464 (1985).

[13] G. J. Feldman and R. D. Cousins, Phys. Rev. D **57** 3873 (1998).

[14] Particle Data Group, C. Amsler *et al.*, Phys. Lett. B **667**, 1 (2008).

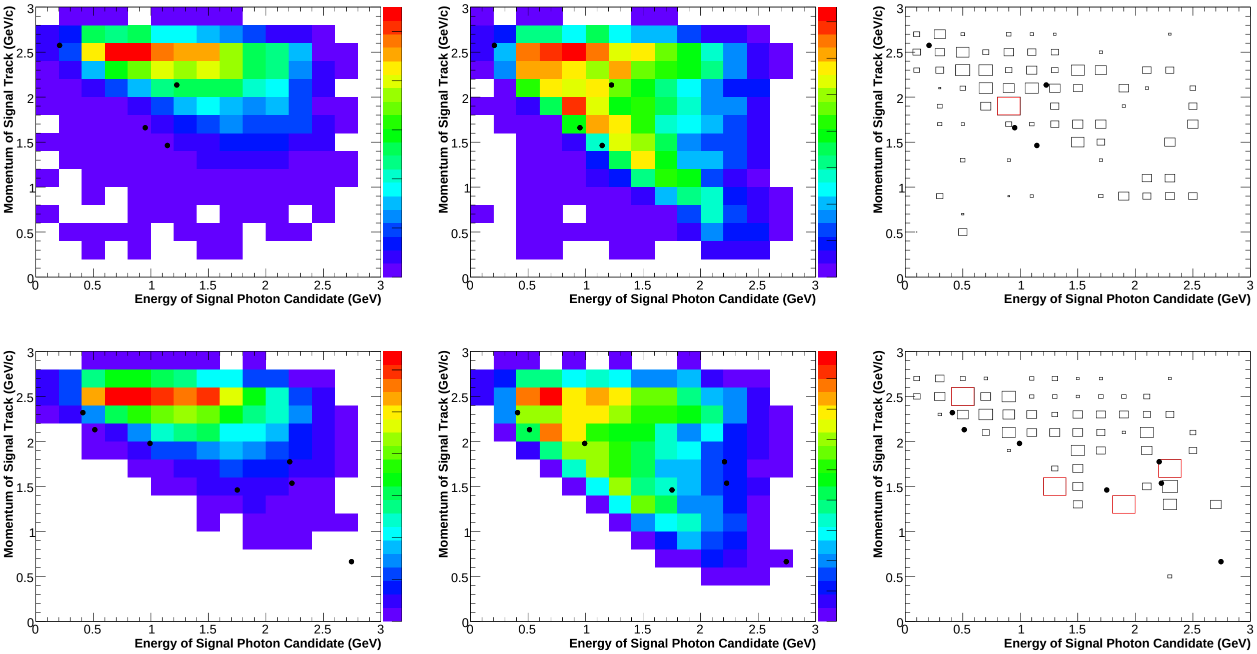

Figure 2: The distribution of the signal track momentum versus the signal photon candidate energy, in the B_{sig} rest frame, after all signal selection criteria is applied, for data (points), $f_A = f_V$ signal model (left), $f_A = 0$ signal model (middle), and N_ℓ^{bkg} (right). The electron modes are shown on the top and the muon modes are on the bottom. The size of the box in the N_ℓ^{bkg} plots is proportional to the number of background events within the histogram bin. The contribution of N_ℓ^{comb}, which is determined using data events in the m_{ES} sideband, is shown as red boxes.

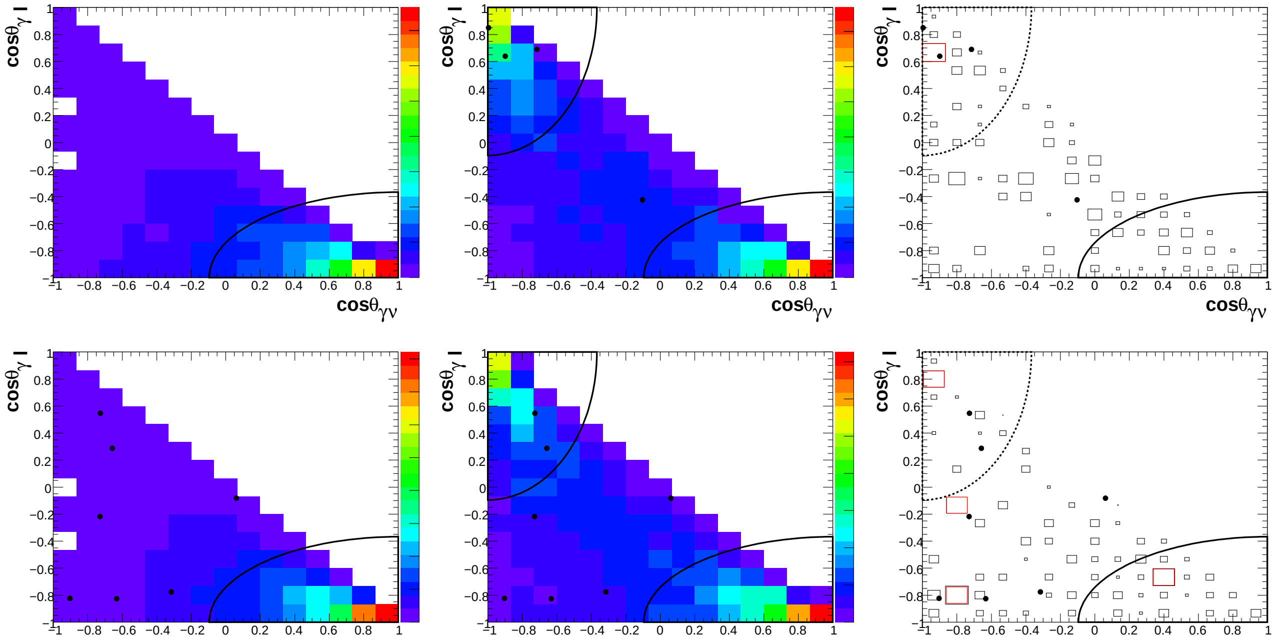

Figure 3: The correlation between $\cos\theta_{\gamma\ell}$ and $\cos\theta_{\gamma\nu}$, in the B_{sig} rest frame, after all signal selection criteria is applied, for data (points), $f_A = f_V$ signal model (left), $f_A = 0$ signal model (middle), and N_ℓ^{bkg} (right). The electron modes are shown on the top and the muon modes are on the bottom. The size of the box in the N_ℓ^{bkg} plots is proportional to the number of background events within the histogram bin. The contribution of N_ℓ^{comb}, which is determined using data events in the m_{ES} sideband, is shown as red boxes. The black arcs indicate the cut-off values for the model-specific requirements.